Dynamics and locomotion of flexible foils in a frictional environment - Appendix

Xiaolin Wang, Silas Alben

December 13, 2017

1 Appendix A: Numerical solution at the first time step

We use a second-order (BDF) discretization for the time-derivative in the numerical method. Since the discretization requires solutions at the two previous time steps, we need to adjust the method at the first step. We give κ_0 and $\partial_t\kappa_0$ as initial conditions. We obtain $\partial_{tt}\kappa_0$ using a central difference scheme with a guess for κ_1, and obtain $\partial_t\zeta_0$ and $\partial_{tt}\zeta_0$ by integrals. Broyden's method is then applied at step 0 to get the correct κ_1 and ζ_1. The regular procedures (described in the main text) can be used after the first step to obtain further κ_n and ζ_n.

2 Appendix B: Zero Friction Model

When the heaving amplitude A is small, the nonlinear foil equation can be linearized as

$$\partial_{tt}y(x,t) = -B\partial_x^4 y, \tag{1}$$

with friction coefficients set to zero. The boundary conditions become:

$$y(0,t) = A\sin(2\pi t),\ \partial_x y(0,t) = 0; \quad \partial_x^2 y(1,t) = \partial_x^3 y(1,t) = 0 \tag{2}$$

and the initial conditions are:

$$y(x,0) = y_0(x), \quad \partial_t y(x,0) = \partial_t y_0(x) \tag{3}$$

This equation can be solved analytically by separation of variables.

We first rewrite the solution in the form $y(x,t) = u(x,t) + v(x,t)$, where $v(x,t) = A\sin(2\pi t)$. Then $u(x,t)$ satisfies a nonhomogeneous equation with homogeneous boundary conditions:

$$\partial_{tt}u(x,t) = -B\partial_x^4 u + 4\pi^2 A\sin(2\pi t). \tag{4}$$

The solution of equation (4) can be represented as a series of eigenfunctions:

$$u(x,t) = \sum_{i=1}^{\infty} A_i(t)\phi_i(x). \tag{5}$$

The eigenfunctions $\phi_i(x)$ correspond to the modes of a cantilevered beam [1]:

$$\phi_i(x) = \cosh(\omega_i x) - \cos(\omega_i x) + \frac{\cosh\omega_i + \cos\omega_i}{\sinh\omega_i + \sin\omega_i}\left(\sin(\omega_i x) - \sinh(\omega_i x)\right), \tag{6}$$

and the eigenvalues are the roots of the nonlinear equation:

$$\cosh(\omega_i)\cos(\omega_i) + 1 = 0. \tag{7}$$

The eigenfunctions are orthogonal, i.e.,

$$\int_0^1 \phi_i(x)\phi_j(x)dx = 0, \quad i \neq j. \tag{8}$$

The time-dependent coefficients $A_i(t)$ therefore satisfy the nonhomogeneous ODEs:

$$\frac{d^2A_i(t)}{dt^2} + \lambda_i A_i(t) = \frac{\int_0^1 \phi_i(x)dx}{\int_0^1 \phi_i^2(x)dx} 4\pi^2 A \sin(2\pi t). \tag{9}$$

where $\lambda_i = B\omega_i^4$, which is also related to the eigenvalues of the vibration system. The solution of the ODE is of the form:

$$A_i(t) = B_i \sin(2\pi t) + C_i \cos(\sqrt{\lambda_i}t) + D_i \sin(\sqrt{\lambda_i}t). \tag{10}$$

By applying equation (9) and the initial conditions (3), we obtain the following coefficients:

$$B_i = \frac{4\pi^2 A \int_0^1 \phi_i(x)dx}{(-4\pi^2 + \lambda_i)\int_0^1 \phi_i^2(x)dx}, \tag{11}$$

$$C_i = \frac{\int_0^1 y_0(x)\phi_i(x)dx}{\int_0^1 \phi_i^2(x)dx}, \tag{12}$$

$$D_i = \frac{1}{\sqrt{\lambda_i}} \left(\frac{\int_0^1 (\partial_t y_0(x) - 2\pi A)\phi_i(x)dx}{\int_0^1 \phi_i^2(x)dx} - 2\pi B_i \right). \tag{13}$$

when $\lambda_i = B\omega_i^4 \neq 4\pi^2$ (not at the resonant peaks). Therefore, the deflection of the linearized model is given by

$$y(x,t) = \sum_{i=1}^{\infty} A_i(t)\phi_i(x) + A\sin(2\pi t). \tag{14}$$

The linearized model approximates the foil deflection well when the amplitude A is small. In figure 1(a), we choose the initial conditions as $y_0(x) = 0.01(-\frac{1}{24}x^4 + \frac{1}{6}x^3 - \frac{1}{4}x^2)$ and $\partial_t y_0(x) = 0.01(-\frac{1}{24}x^4 + \frac{1}{6}x^3 - \frac{1}{4}x^2) + 2\pi A$ and compare the trailing edge (free end) displacement computed by the numerical simulation and the linearized model until $t = 20$. The other parameters used here are $A = 0.01$ and $B = 1$. In figure 1(b), we plot the spectrum of the frequency based on the free end displacement. The simulation and the analytical results agree well. The coefficients A_i

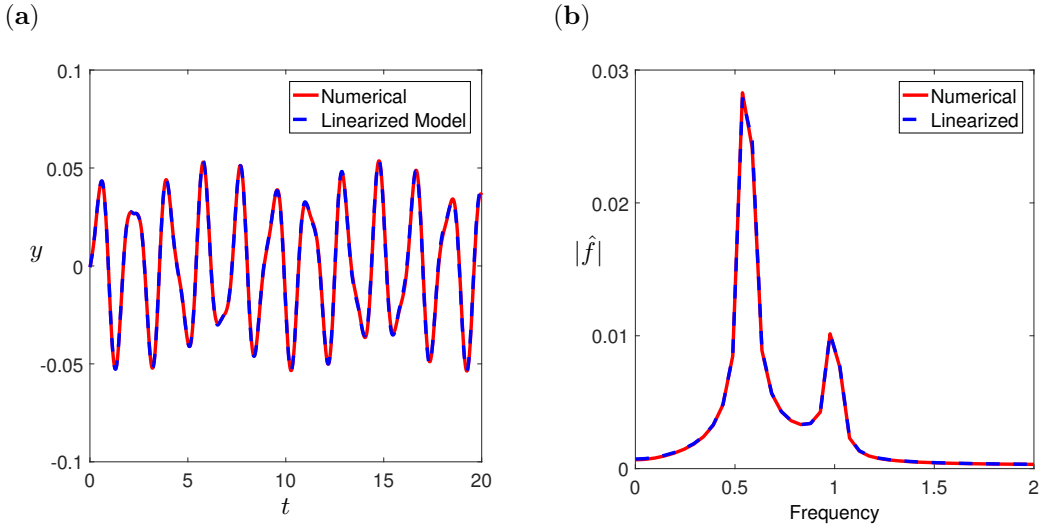

Figure 1: (a). Free end displacement y vs. time t. The solid line denotes the numerical simulation result, and the dashed line denotes the analytical result for the linearized model for $A = 0.01$ and $B = 1$. (b) Corresponding spectrum amplitude $|\hat{f}|$ vs. frequency.

converge to zero quickly, and the first natural vibration mode dominates as shown in the frequency spectrum plot.

Since the coefficients C_i and D_i depend on the initial conditions, we can choose $y_0(x)$ and $\partial_t y_0(x)$ such that $C_i = D_i = 0$. For example, $y_0(x) = 0$, and $\partial_t y_0(x) = \sum_{i=1}^{\infty} 2\pi B_i \phi_i(x) + 2\pi A$.

Therefore, the foil deflection for the linearized model becomes periodic in time as $y(x,t) = \sum_{i=1}^{\infty} B_i \sin(2\pi t)\phi_i(x) + A\sin(2\pi t)$. As we increase the magnitude A, nonlinearity is introduced into the system and the periodicity will be broken. In figure 2, we apply the initial conditions as discussed above, and compare the spectrum of the frequency based on the free end displacement for the linearized model and the numerical simulation. We observe another frequency spectrum which corresponds to the first natural frequency ω_1 as A increases for the numerical results.

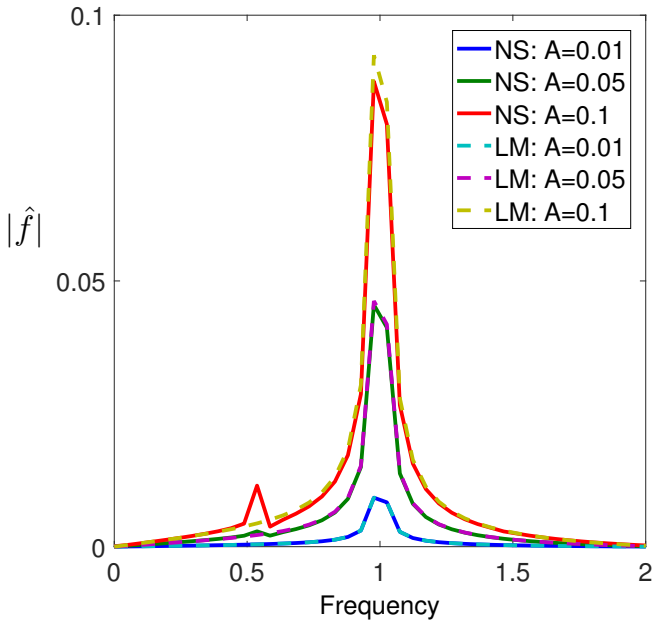

Figure 2: Spectrum amplitude $|\hat{f}|$ vs. frequency based on free end displacement. The solid lines denote the numerical simulation results, and the dashed lines denote the analytical linearized model for $B = 1$ and various $A = 0.01, 0.05$ and 0.1.

References

[1] Alper Erturk and Daniel J Inman. On mechanical modeling of cantilevered piezoelectric vibration energy harvesters. *Journal of Intelligent Material Systems and Structures*, 19(11):1311–1325, 2008.